

Article (refereed) - postprint

Smith, D. Scott; Nasir, R.; Parker, Wayne; Peters, A.; Merrington, G.; van Egmond, R.; Lofts, S. 2021. **Developing understanding of the fate and behaviour of silver in fresh waters and waste waters.**

© 2020 Elsevier B.V.

This manuscript version is made available under the CC BY-NC-ND 4.0 license
<https://creativecommons.org/licenses/by-nc-nd/4.0/>



This version is available at <https://nora.nerc.ac.uk/id/eprint/529043/>

Copyright and other rights for material on this site are retained by the rights owners. Users should read the terms and conditions of use of this material at <https://nora.nerc.ac.uk/policies.html#access>

This is an unedited manuscript accepted for publication, incorporating any revisions agreed during the peer review process. There may be differences between this and the publisher's version. You are advised to consult the publisher's version if you wish to cite from this article.

The definitive version was published in *Science of the Total Environment* (2021), 757. 143648. <https://doi.org/10.1016/j.scitotenv.2020.143648>

The definitive version is available at <https://www.elsevier.com/>

Contact UKCEH NORA team at
noraceh@ceh.ac.uk

1 Developing Understanding of the Fate and Behaviour of Silver in Fresh 2 Waters and Waste Waters

3 D. Scott Smith^{a,*}, R. Nasir^a, Wayne Parker^b, A. Peters^c, G. Merrington^c, R. van Egmond^d, S. Lofts^e

4 ^a Department of Chemistry and Biochemistry, Wilfrid Laurier University, Waterloo, ON, CANADA

5 ^b Department of Civil and Environmental Engineering, University of Waterloo, Waterloo, ON, CANADA

6 ^c WCA Environment Ltd., Brunel House, Faringdon, Oxfordshire, UK

7 ^d Safety and Environmental Assurance Centre, Unilever, Sharnbrook, Bedfordshire, United Kingdom

8 ^e Centre for Ecology and Hydrology, Lancaster Environment Centre, Library Avenue, Bailrigg, Lancaster LA1 4AP, United Kingdom

10 Abstract

11
12 The Windermere Humic Aqueous Model (WHAM) is often used for risk assessment of
13 metals; WHAM can be used to estimate the potential bioavailability of dissolved metals,
14 where metals complexed to dissolved organic matter (DOM) are expected to be less toxic
15 than ionic forms. Silver is a potential metal of concern but WHAM has not been rigorously
16 tested against experimental measurements. This study compares WHAM predictions to
17 measured ionic silver during fixed pH (4, 8 or 10) argentometric titrations of DOM from
18 diverse origins. There were almost two orders of magnitude variation in free silver between
19 sources but, within model uncertainty, WHAM captured this variability. This agreement,
20 between measurements and models, suggests that WHAM is an appropriate tool for silver
21 risk assessment in surface receiving waters when DOM is predominantly in the form of
22 humic/fulvic acids. In sewage samples WHAM dramatically underestimated silver binding by
23 approximately 3 orders of magnitude. Simulations with additional specific sulphide-like
24 binding sites could explain Ag binding at low loadings, but not at higher loadings. This
25 suggests the presence of additional intermediate strength binding sites. These additional
26 ligands would represent components of the raw sewage largely absent in natural waters
27 unimpacted by sewage effluents. A revised empirical model was proposed to account for
28 these sewage-specific binding sites. Further, it is suspected that as sewage organic matter is
29 degraded, either by natural attenuation or by engineered treatment, that sewage organic
30 matter will degrade to a form more readily modelled by WHAM; i.e., humic-like substances.
31 These ageing experiments were performed starting from raw sewage, and the material did in
32 fact become more humic-like, but even after 30 days of aerobic incubation still showed
33 greater Ag⁺ binding than WHAM predictions. In these incubation experiments it was found
34 that silver (up to 1000 µg/L) had minimal impact on ammonia oxidation kinetics.

35
36 Keywords: silver, Windermere Humic Aqueous Model (WHAM), ion selective electrode,
37 sulphide binding sites, risk assessment, metal bioavailability

38

39 Introduction

40 Exposures to ionic silver are known to result in adverse effects in laboratory test organisms
41 at concentrations in the sub microgram per litre range (Hogstrand et al., 1996; Peters et al.,
42 2011). Yet, environmental exposures are rarely in the ionic form and so are likely to be less
43 ecotoxicologically potent (Johnson et al., 2014). Silver can bind to inorganic ligands such as
44 chloride and sulphide, as well as binding to organic ligands such as dissolved organic matter
45 (DOM). An understanding of the chemical form, or speciation, of environmental exposures of
46 silver is critical in assessing the potential risks from silver uses. A developed understanding
47 of the chemical behaviour in an environmental matrix is critical in predicting potential
48 bioavailability (e.g. Brauner and Wood (2002)). It is widely recognised that bioavailability, as
49 a reflection of the exposure of a metal that the organism experiences, delivers the most
50 biologically relevant metric by which to assess potential risk in soils, sediments and waters.
51 Metals, such as nickel and lead, have European wide “bioavailability” based environmental
52 quality standards (EQS)(European Commission (EC), 2013, 2018) and for copper and zinc
53 national bioavailability-based EQS are also available in some countries (e.g. Environment
54 Agency (2009)). It has long been established that water chemistry and especially dissolved
55 organic carbon (DOC) and sulphur compounds in freshwater and effluents can bind with
56 silver, mitigating ecotoxicity and influencing its behaviour and fate (Di Toro et al., 2001;
57 Hiriart-Baer et al., 2006). Despite recognising the importance of water chemistry upon silver
58 in freshwaters regulatory efforts to incorporate this understanding into EQS setting are lacking
59 (Sahlin and Ågerstrand, 2018).

60 Silver has been identified as a potential substance for prioritisation as a potential EU-wide
61 EQS. One of the lines of evidence used to facilitate this risk-based prioritisation is the
62 consideration of measured national silver exposures. Unfortunately, these data are difficult
63 to interpret, as measured silver data in fresh and marine waters are often below detection;
64 for example, in Carvalho et al. (2016), less than 9% of the more than 13,000 samples were
65 quantifiable. Trying to handle “non-detects”, renders the summary statistics used for the risk-
66 based approach extremely uncertain (Hites, 2019).

67 Ionic silver is known to have antimicrobial properties and is utilized in biocides, medical
68 applications and commercial personal-care products for this purpose (Wakshlak et al.,
69 2015); for similar reasons the use of silver nanoparticles has also increased, such as in
70 treated clothing (Emam et al., 2013). Thus, there is potential for silver input to the
71 environment, e.g., via municipal wastewater treatment effluents. With the increased discharge
72 of silver to the environment, it is necessary to have in place methods to assess the risk of
73 silver in aquatic environments.

74 There are many approaches to assessing the risks posed by discharges of silver into the
75 environment. Bioavailability based approaches take the reactivity of different chemical forms
76 of an element into account; the most bioavailable forms are expected to have greater
77 toxicity. Such approaches have been useful in setting appropriate and protective regulatory
78 guidelines for some other metals, such as aluminum, cadmium, cobalt, copper, nickel, lead
79 and zinc (Adams et al., 2019). To properly accomplish this for silver, the greatest current
80 data gap is a detailed understanding of the role of reduced sulfide in silver binding, and
81 ultimately in toxicity mitigation by decreasing the concentrations of potentially toxic
82 bioavailable forms of silver. It is well understood that silver binds strongly to reduced sulfide
83 ligands but measuring sulfide is not part of routine analysis when characterizing samples for
84 risk assessment purposes. Even with sulfide data, there do not currently exist validated
85 computer models to estimate bioavailability from measured water chemistry (i.e.,
86 measurements such as dissolved organic carbon (DOC), pH, major cations, major anions,
87 inorganic sulfide and organic sulfide (thiol)). Thus, regulated industries do not yet have
88 sufficient information or tools to make appropriate risk-based management decisions for Ag
89 in the environment. There is a need to improve the understanding of the behaviour and fate
90 of silver in environmental systems in order to ensure decisions in regard to potential risk and
91 environmental stewardship are evidence-based.

92 It is the aim of the work described in this paper to determine the chemical availability of silver
93 in natural freshwater and specifically improve the understanding of silver fate and behaviour
94 to facilitate a scientific evidence driven approach to environmental risk assessment.
95 Chemical speciation models, such as the Windermere Humic Aqueous Model (WHAM,
96 (Tipping et al., 2011)), have been widely used in the derivation and implementation of water
97 quality standards for metals such as copper, nickel and zinc in Europe (e.g. Merrington et al.
98 (2016)). The silver data upon which WHAM is calibrated (see Supplementary Material
99 associated with Tipping et al. (2011) available at
100 http://www.publish.csiro.au/en/acc/EN11016/EN11016_AC.pdf) is limited to two studies
101 (Sikora and
102 Stevenson, 1988; Rader et al., 2005); therefore, delivering a greater understanding of silver
103 behaviour in freshwater requires improvement in the basis of the predictions, and
104 subsequent validation of the model for silver. In addition, it is recognized that different sources
105 or dissolved organic matter may have different binding characteristics with metals (Al-Reasi
106 et al., 2011b), thus a diversity of sources are studied here, including treated wastewater
107 effluents. Finally, a range finder toxicity test was performed to determine the impact of silver
108 on the natural attenuation treatment of wastewater; i.e., addressing whether or not silver
109 impacts the kinetics of nitrogen oxidation in raw sewage.

110
111 2. Methods

112 2.1. Silver Ion Selective Electrode Titrations

113 The silver electrode is one of the most sensitive of the solid-state ion selective electrodes
114 (ISE). There has been limited work titrating NOM samples using a silver ISE though (Sikora
115 and Stevenson, 1988; Smith et al., 2004). Initial efforts for this study involved establishing
116 best practices for silver ISE titrations and best operating conditions. Experimental methods
117 requiring optimization included the calibration method (internal or external) as well as the
118 sample exposure method (flow through or static). The titration curves in this report were all
119 obtained using internal standard calibration and flow through ISE. This decision was based
120 on best recovery of known [Ag⁺] values for silver titration of EDTA
121 (ethylenediaminetetraacetic acid). The EDTA titration data are presented in the
122 Supplemental Material associated with this manuscript (Figure S11).

123 A Cole Parmer Silver/Sulfide ISE was utilized for all experiments with an Orion double
124 junction Ag/AgCl reference electrode (Model 900200, Boston, MA, USA). For flow through
125 experiments a micro-Flowcell (FIALab, Bellevue, WA) was utilized. Each electrode was
126 connected to a potentiometer (Tanager, Model 9501, Ancaster, ON). For flow through
127 experiments a valveless metering pump, the Cerampump FMI “Q” Pump (GQ6, Fluid
128 Metering Inc., Syosset, NY) was used to deliver the test solution through the system. This
129 type of pump was found not to interfere with the low current flow potential measurements of
130 the electrode.

131 The potential (E) of the silver ion selective electrode responds to free silver ion concentration
132 ([Ag⁺]) according to the Nernst equation:

133
134
$$E = E_0 + m \log [\text{Ag}^+] \tag{1}$$

135

136 Equation 1 was used to calibrate the electrode in order to convert measured potentials into
137 [Ag⁺] values. At 25 °C, the Nernstian slope (m) typically has a value of 59.2 mV/decade of
138 concentration for monovalent ions such as silver. For this study, an internal one-parameter
139 calibration was used to determine E₀, the intercept of the calibration line; the theoretical
140 Nernstian value for the slope in Equation (1) was assumed. All samples had intrinsic or
141 added chloride ions, and once enough silver had been added during titration, the ion product
142 for solid silver chloride would exceed the K_{sp} value and solid would precipitate. The presence
143 of solid AgCl buffers the free silver ion and the electrode potential will remain constant. This
144 constant mV response was used to solve for E₀ in Equation (1), again assuming a Nernstian
145 slope. In order to perform this operation the [Ag⁺] in this “buffered zone” must be determined.

146 This is accomplished assuming the only relevant species are $\text{AgCl}_{(s)}$, Ag^+ and Cl^- ; using
147 these species the mass balance and mass action equations can be written in terms of $[\text{Ag}^+]$
148 as the only variable:

$$149 \quad [\text{Ag}^+]^2 + (\text{Cl}_T - \text{Ag}_T)[\text{Ag}^+] - K_{sp} = 0 \quad (2)$$

151 Equation 2 can be solved (e.g., by root finding) to determine $[\text{Ag}^+]$, using the measured total
152 chloride in the sample (Cl_T), and the known total silver added at the end of the titration (Ag_T).
153 The simplified speciation during the calibration is valid as long as the chloride concentration
154 is much higher than other potential ligands (i.e., DOC) in the sample. A similar one-
155 parameter internal standard method has been successfully utilized for a copper ion selective
156 electrode in salt water (Tait et al., 2015).
157

158 2.2. Sample collection and characterization

159 Sample locations, and types of organic matter sources, utilized in this study are summarized
160 in Table 1. Dissolved organic matter (DOM) was collected using a portable reverse osmosis
161 (RO) unit. For details on reverse osmosis, see Sun et al. (1995), and previous publications
162 using the same RO system and sample locations (Al-Reasi et al., 2011a). The prefilter on
163 the RO unit was a 1 μm wound string filter. Dark, terrigenous (allochthonous) DOM was
164 collected from Luther Marsh, while mixed autochthonous/allochthonous DOM was collected
165 from Bannister Lake. Sewage-derived NOM samples were collected from the effluent of the
166 Dundas Sewage Treatment Plant, as well as Burlington Bay, where effluent mixes with
167 autochthonous carbon from Lake Ontario. Finally, raw sewage (i.e., not RO concentrates)
168 from the University of Waterloo, and at Ashbridges Bay treatment plant in Toronto were
169 collected. The University of Waterloo sewage is municipal sewage collected by means of a
170 sump pump inside the sewer. Two reference NOM samples, Suwanee River and Nordic
171 Reservoir, both obtained from the International Humic Substances Society (IHSS), were also
172 used for silver titrations. All RO samples were stored in a cold room at 4 $^{\circ}\text{C}$ until use.
173 Titrations were performed using approximately 100 mg C L^{-1} . The actual DOC concentration
174 in titrated samples are indicated in Table 2, as well as measured total chloride concentration.
175 For each sample at least one replicate titration was performed. Initial testing demonstrated
176 that lower concentrations of DOC did not show sufficiently low detection limit to “probe”
177 strong binding sites and higher concentrations resulted in lower binding site estimates per
178 mg of carbon. It is suspected that at high DOC concentrations DOM-DOM interactions
179 remove binding sites from availability towards silver, as has been observed before for lead
180 and copper (Nadella et al., 2013; Cooper et al., 2014). It should be noted that the RO
181 procedure concentrates all components of the initial sample so inorganic ligands (i.e.,

182 chloride) are elevated in addition to DOC. The RO concentrates are still representative of
 183 natural samples; although the ligand concentrations are elevated for analytical reasons, the
 184 carbon to chloride ratio is the same in the concentrate as in the original source water. To
 185 remove potential metal contamination, the reverse osmosis-derived NOM concentrates from
 186 each site were passed through a cation exchange resin (Amberlite IR-118H, Sigma),
 187 acidified (pH 2), and then stored in the dark, at 40°C, in 4L polyethylene bottles until used in
 188 experiments or analysed (e.g. Schwartz et al. (2004); Winter et al. (2007)).

189 Table 1. Samples used in this study

Code	Name	Coordinates	Comment
SR	Suwannee River NOM	obtained from IHSS	reference NOM
NR	Nordic Reservoir NOM	obtained from IHSS	reference NOM
LM	Luther Marsh	43°54'17.5"N 0.0°24'34.9"W	allochthonous
BL	Bannister Lake	43°17'34.7"N 080°23'14.0"W	mixed autochthonous/allochthonous
BB	Burlington Bay	43°18'03.3984"N 079°50'33.8280"W	mixed sewage/autochthonous
DC	Dundas Canal	43°15'59.2308"N 080°32'19.5576"W	sewage effluent
UW	University of Waterloo	43°28'14.5092"N 080°32'19.5576"W	raw sewage
AB	Ashbridges Bay	43°39'25.6"N 079°19'15.0"W	raw sewage

190
 191 Organic thiol was quantified using a fluorometric thiol assay kit (MAK151-1KT, Sigma
 192 Aldrich, Toronto, ON, Canada). Measurements were performed using a SpectraMAX Gemini
 193 XS microplate reader (Molecular Devices, Sunnyvale, CA, USA). Chromium reducible
 194 sulphide (CRS) was measured using the method originally developed by Bowles et al.
 195 (2003). The method was slightly modified in that Cr(II) was purchased directly from Sigma-
 196 Aldrich (Toronto, ON, Canada) instead of being generated from Cr(III) salt using a Jones
 197 Reductor column (i.e., mercury and zinc amalgam). To ensure high quality data several
 198 sulphide standards were run and 500, 1000 and 2000 nM standards gave 96.7, 97.7, 103 %
 199 recoveries respectively.

200 Absorbance and fluorescence spectroscopy have frequently been successfully employed to
 201 distinguish the molecular variability among natural samples from various sources, as well as
 202 between fulvic and humic acids from the same source. Optical properties such as the
 203 specific absorbance coefficient, SAC (estimated as 2.303 × absorbance at a specific

204 wavelength, often 340nm and, normalized to TOC) (Curtis and Schindler, 1997) and the
205 fluorescence index (FI, determined as fluorescence intensity at 450 nm/fluorescence
206 intensity at 500 nm; both taken at excitation wavelength of 370 nm) (McKnight et al., 2001)
207 have been reported to distinguish NOM sources and composition. Fluorescence
208 measurements were performed with a Cary Eclipse fluorescence spectrophotometer
209 (Agilent, Toronto, ON, Canada) and absorbance spectra were measured using Cary 50 Bio
210 spectrophotometer (Agilent, Toronto, ON, Canada). For all optical measurements 1 cm
211 quartz cuvettes (Starna Cells, Inc. Atascadero, CA, USA, model 3-Q-10) were utilized.

212 The total DOC concentration was measured directly using a Shimadzu TOC-VCPH/CPN
213 total organic carbon analyzer (Shimadzu Corporation, Kyoto, Japan). The reproducibility of
214 the TOC analyzer using standard total carbon solutions of 5 and 10 mg L⁻¹ (prepared from
215 primary standard potassium hydrogen phthalate (KHP)) yielded 5.26 ± 0.66 mg C L⁻¹ (n =
216 44) and 10.24 ± 0.43 mg C L⁻¹ (n = 77). Chloride was determined using a chloride ion
217 selective electrode (Chloride ionplus Sure-Flow Solid State Combination ISE, Thermo
218 Scientific) calibrated using NaCl solutions in the range 1.00 µM to 0.0100 M.

219 2.3. Speciation Modelling

220 Speciation modelling was performed using WHAM7 (Tipping et al., 2011). Data analysis and
221 plotting was performed utilizing Matlab R2019a (MathWorks , Natick, MA, USA) including the
222 statistics toolbox for regression analysis.

223 2.4. Sewage Incubation Experiments

224 Raw sewage obtained from the University of Waterloo (UW) was used for two incubation
225 experiments while the total chloride concentration was low enough to add sufficient silver to
226 avoid AgCl precipitation. For unknown reasons, possibly due to road-salt additions, the UW
227 source dramatically increased in chloride concentration, and Ashbridges Bay (AB) from
228 Toronto was used for a third incubation experiment. These experiments were intended as
229 “range finder” experiments to see if high concentrations of added silver would have any
230 negative impacts on the potential treatment of sewage using natural attenuation process; in
231 particular, the oxidation of more toxic ammonia to less toxic nitrate. The ammonia used in
232 these experiments was just the ambient ammonia originally present in the sample. There
233 was no spiking of additional ammonia. For each nominal dose of silver, 3 L of unfiltered raw
234 wastewater was incubated in a fume hood, with aeration and constant temperature of 24 ±
235 2°C for approximately 30 days. For each dose there were two replicate 4 L graduated glass
236 bottles. The sewage samples were aerated using air pumps and air stones; the bubbles also
237 provided mixing. Every day evaporative losses were replaced using deionized water. During
238 the course of the experiment ammonia, nitrite and nitrate were measured in filtered samples

239 from the treatments, using Hach kits and a Hach spectrometer (DR3900 Hach
240 Spectrophotometer). Subsamples were taken for DOC analysis (for method see above,
241 including 0.45 μm filtration) as well as dissolved silver analysis. Dissolved silver was
242 determined by graphite furnace atomic absorption spectroscopy (Perkin Elmer PinAAcle
243 900T AA). Experimental setup is shown in Figure SI2 and SI3 for clean water setup testing
244 and actual sewage incubations, respectively.

245 3. Results and Discussion

246 3.1. Sample Characteristics

247 The samples span a range of quality parameters (Table 2). Chloride was highest in the BB
248 and DC samples impacted by sewage effluent. This limited the upper end of the titration
249 range, as AgCl(s) precipitation would begin at lower total silver concentrations. Chromium
250 reducible sulfide normalized to DOC spanned more than an order of magnitude in
251 concentration with values as low as 2.7 nmol CRS/mg C for the terrigenous NR sample and
252 up to 95 for the UW sewage sample. Thiol concentrations spanned a much lower range with
253 the sewage impacted BB sample actually being the lowest (44 nmol/mg C) and the highest
254 being the other sewage impacted sample approximately 3X higher (138 nmol/mg C). The
255 two estimates of reduced sulphur measure different things. CRS does not respond to organic
256 thiol and measures only inorganic reduced S, such as in colloidal metal sulphides (Bowles et
257 al., 2003). The thiol assay only measures the organic thiol group content. The ionic silver
258 measured at the Ag_T/DOC *Ceriodaphnia dubia* EC50 value (Naddy et al., 2017) spans
259 almost 4 orders of magnitude with UW showing the lowest value ($10^{-11.8}$ M) and NR the
260 highest value ($10^{-8.12}$ M). In terms of metal complexation, as long as the complex is assumed
261 to be 1:1, it is the metal to ligand ratio that determines the fraction of metal that is complexed
262 by DOM. For this reason, the total added silver for each titration is presented normalized to
263 the corresponding DOC value for that sample.

264 As expected, the SAC340 values were highest for the most terrigenous samples (LM, SR,
265 NR) all with values near 30, and the more autochthonous and/or sewage samples (BL, BB,
266 DC) with values closer to 10. Similarly the FI values clearly demarcated the same more
267 autochthonous samples with the lowest values from the higher value autochthonous
268 samples. The results of the absorbance and fluorescence optical characterizations are
269 consistent with previous surveys of SAC340 and FI (Al-Reasi et al., 2011b). Original
270 fluorescence excitation emission matrices (FEEMs) are presented in Figure SI4. These
271 scans demonstrate the typical terrigenous shapes (two excitations around 250 and 350 with
272 emission around 450 representing humic substances) for the NR and SR samples. The
273 mixed source DC and BB and BL sources show more autochthonous characteristics with

274 shorter wavelength fluorescence peaks indicating proteinaceous material. The sewage
 275 sample (UW) showed the greatest proportion of protein-like fluorescence at these shorter
 276 wavelengths with the largest emission at wavelengths very similar to tryptophan (i.e.,
 277 excitation around 240 nm and excitation at 350 nm). In the supplementary information table
 278 SI1 summarizes the usually reported parameters specific to the UW wastewater sample.

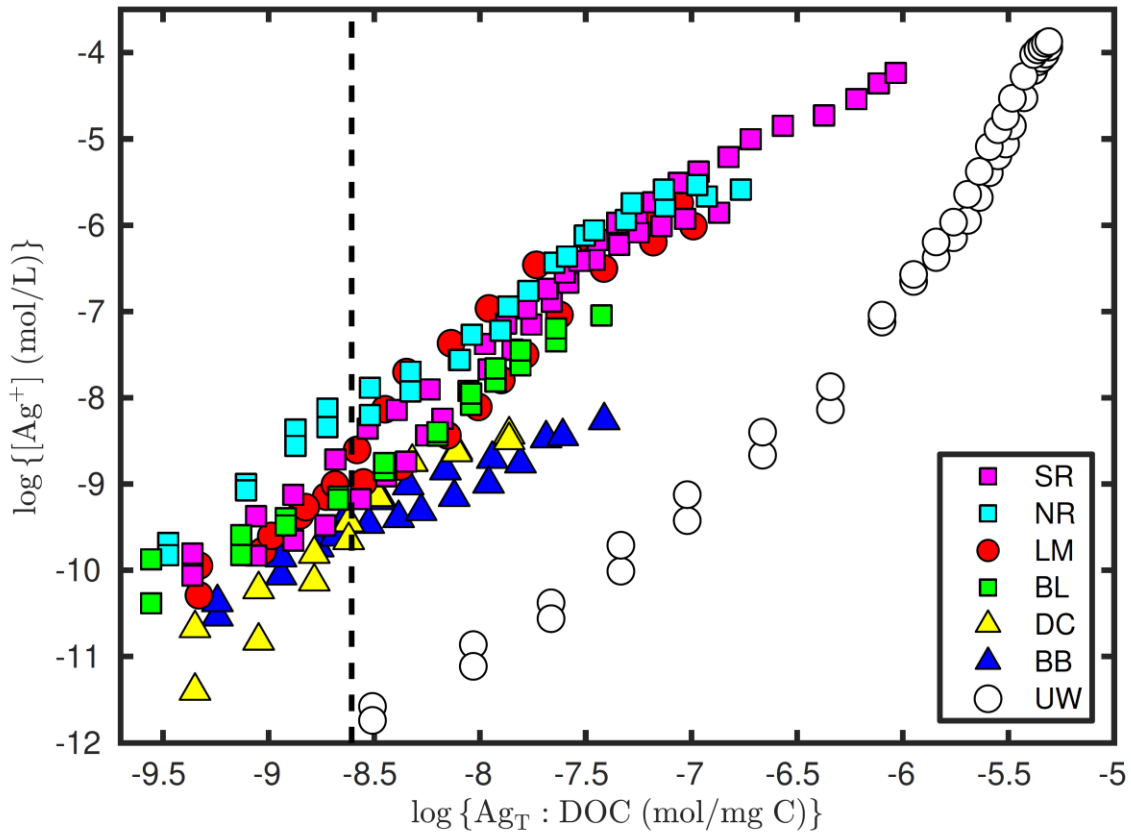
279 Table 2: Sample optical and chemical characterization. *a* DOC of titrated samples. *b* the
 280 logarithm of the silver ion concentration measured at the $Ag_T:DOC$ ratio equivalent to the
 281 *Ceriodaphnia dubia* EC50 value measured by Naddy et al. (2017). Uncertainties reported as
 282 standard deviations on duplicate measurements. The “-” symbols indicate missing data
 283 where the samples were not measured.

Code	DOC ^a mg/L	Chloride μmol/mg C	CRS nmol/mg C	Thiol nmol/mg C	SAC ₃₄₀	FI	log[Ag ⁺] ^b
SR	85	3.0	4.28±0.57	120±9	28.1	1.04	-8.89±0.52
NR	89	6.0	2.69±0.01	72±40	30.7	1.14	-8.12±0.20
LM	99	9.0	2.85±0.23	117±1	36.6	1.00	-8.87±0.23
BL	83	40	8.10±1.02	109±18	11.6	1.38	-9.07±0.01
BB	81	600	7.49±2.52	41±50	8.43	1.42	-9.45±0.12
DC	62	600	12.73±0.80	138±65	11.9	1.49	-9.51±0.13
UW	30	5.0	94.90±7.55	-	-	-	-11.80±0.09
AB	35	11.4	80.8	-	-	-	-11.78±

284

285 3.2. Fresh and wastewater DOM source titrations

286 As indicated in the methods section, all titrations were performed using internal standard
 287 calibration and flow through ISE. This decision was based on best recovery of known [Ag⁺]
 288 values for silver titration of EDTA (ethylenediaminetetraacetic acid). See supplemental
 289 information, Figure SI1 for EDTA model ligand titrations. Silver titration curves of samples
 290 are presented in Figure 1. Titration curves are shown with the total silver added normalized
 291 to DOC to correct for the slight differences between actual DOC concentrations in each
 292 titrated sample (Table 2). The various surface water samples cluster together with a range of
 293 approximately two orders of magnitude in free silver. The samples with the most wastewater
 294 character (DC and BB) tend to be at the low end of the free silver range and the more
 295 allochthonous samples (NR, SR and LM) tend towards the highest values for free silver. The
 296 raw wastewater sample shows much stronger silver binding than the other samples with free
 297 silver four orders of magnitude lower than for the allochthonous sources (Figure 1).

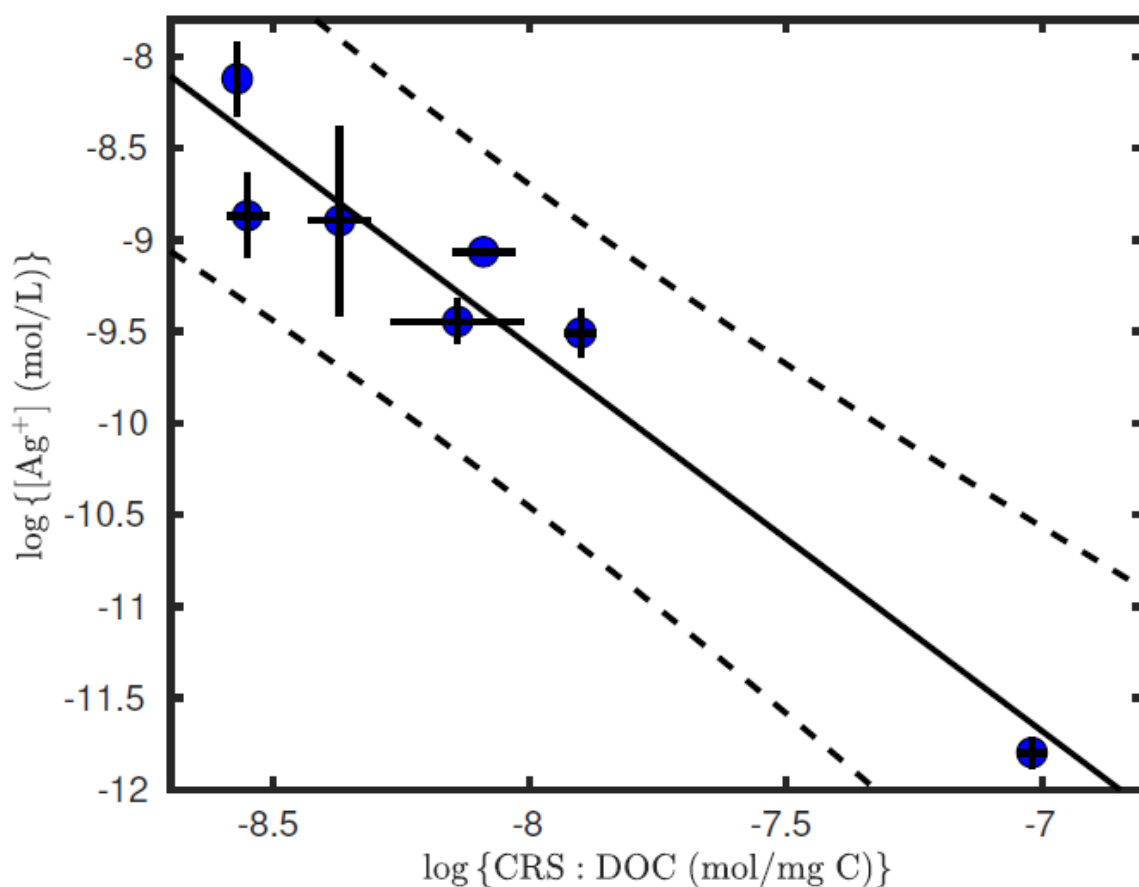


298

299 Figure 1: Silver titration data for DOM samples at pH 8.0 with 0.01 M ionic strength (KNO₃).
 300 Colours and symbols for each sample code given in Table 1 are shown in the figure legend.
 301 The vertical dashed line corresponds to the *Ceriodaphnia dubia* EC₅₀ value measured by
 302 Naddy et al. (2017)

303 The reproducibility of the individual titrations can be seen by comparison of the duplicate
 304 values for each source. The range of free silver spanned by all the samples is much greater
 305 than the range for each individual source (typically 0.2 orders of magnitude or less). The
 306 higher Cl samples (DC, BB, BL) were limited at the upper titration range due to AgCl(s)
 307 precipitation. Low Cl samples such as NR and SR could be titrated to much higher total
 308 silver concentrations. Despite being performed at high DOC, these titrations, with DOC
 309 normalization, span an environmentally reasonable range of concentrations given 202 that
 310 there are measured values above and below the sensitive, and regulatory relevant, effect
 311 concentration for the freshwater invertebrate *Ceriodaphnia dubia* (dashed line in Figure 1).
 312 This value corresponds to the lowest EC₅₀ value measured in Naddy et al. (2017), 0.16 µg
 313 Ag/L at a DOC of 0.5 mg C/L. The range of silver speciation data is two orders of magnitude
 314 in free silver for the surface water samples and up to four orders of magnitude including the
 315 sewage sample. It should be possible to use a measure of quality to inform modelling to
 316 capture this variability. This has been done previously in copper biotic ligand modelling using

317 SAC340 or spectrally resolved fluorescence components to improve the estimates of %fulvic
 318 and %humic acid WHAM inputs (Al-Reasi et al., 2011b; De Schampelare et al., 2004). To
 319 test whether various measures of organic matter quality correlate at all with measured silver
 320 speciation, the free silver ion measured at the DOC normalized *C. dubia* EC50 for each
 321 sample was regressed against each quality measure for the same samples. Results are
 322 reported in Table S12 of the supplemental information. The only significant correlation was
 323 with the log (base 10) of DOC normalized CRS concentrations. These results are shown in
 324 Figure 2. The potential significance of CRS to help predict silver speciation is discussed
 325 further in the modelling section below.

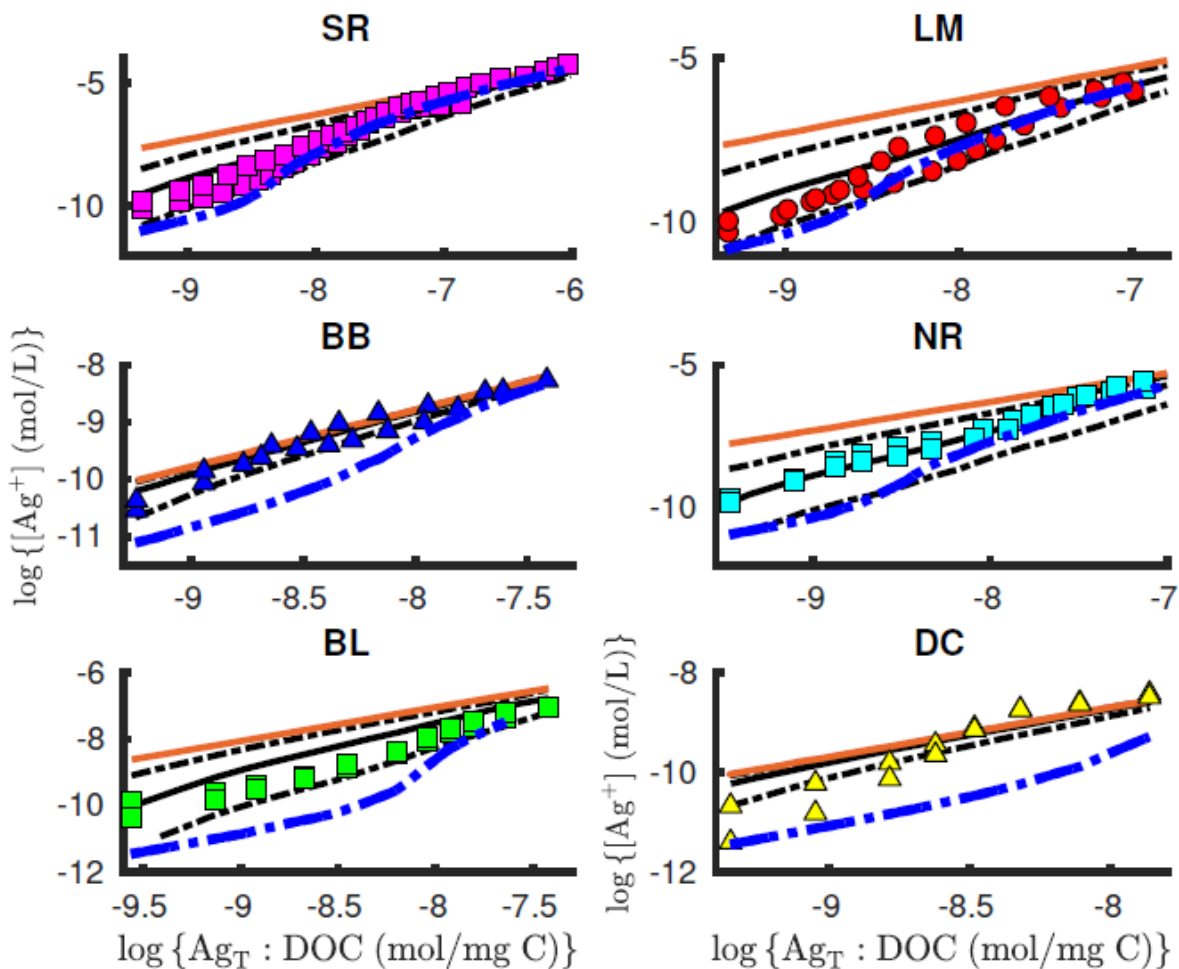


326
 327 Figure 2: Relationship between CRS and free silver at *Ceriodaphnia dubia* 48 hour LC50
 328 value (Naddy et al., 2017). The r^2 for the relationship with all 7 data points included is 0.936
 329 (p value < 0.001), excluding the high CRS UW sample the r^2 value is 0.704 (p value 0.036).
 330 Error bars represent standard deviation on duplicate measurements.

331 3.3. WHAM modelling

332 Figure 3 shows WHAM predictions for all the DOM samples at pH 8.0, with the exception of
 333 the WS raw sewage sample, which is treated separately below. For the SR, LM, NR and BL
 334 samples, the observed Ag complexation is within the range predicted by the WHAM model

335 when uncertainty is taken into account. WHAM prediction uncertainty was calculated using
336 an absolute uncertainty of ± 0.3 in the Ag binding constant ($\log K_{MA}$) (Lofts and Tipping, 2011;
337 Ahmed et al., 2013). For the sewage effluent impacted, high chloride, samples BB and DC,
338 the model predicts that most of the complexation is in fact due to the residual chloride
339 present. Although, in both cases, the predictions with DOC present are better than those
340 with only chloride present. In the case of DC, complexation at $\log \text{Ag:DOC}$ ratios below ~ 8.5
341 is greater than the range predicted by the model. Within the estimated uncertainty
342 envelope, WHAM including DOC and chloride complexation, predicts silver speciation for a
343 range of surface freshwater DOM samples, even for environments including some sewage
344 effluent input. Figure 4 shows the corresponding WHAM predictions for samples SR, LM and
345 DC at pH 4.0, 6.0 and 10.0. Predicted binding behaviour at pH 4.0 and pH 6.0 is reasonable
346 (i.e., for the most part the data agrees with model predictions), although binding is somewhat
347 underestimated for sample LM at pH 6.0. Binding at pH 10.0 differs for samples SR and LM;
348 SR shows stronger binding than is predicted by WHAM, while LM binding shows a different
349 trend to that predicted, being similar at low Ag loading, yet stronger than predicted by the
350 model at high loading. Binding to sample DC is well predicted at all the pH values, due to the
351 dominance of binding by the high concentration of chloride in the sample. Again, similar to
352 pH 8 predictions, for surface water DOM sources WHAM predicts, within model uncertainty,
353 silver speciation reasonably well. For high pH, outside the range of normal waters, the model
354 does underpredict binding, but for risk assessment the underprediction of binding is
355 conservative; thus, WHAM would still be an appropriate tool to help inform water
356 management decisions.

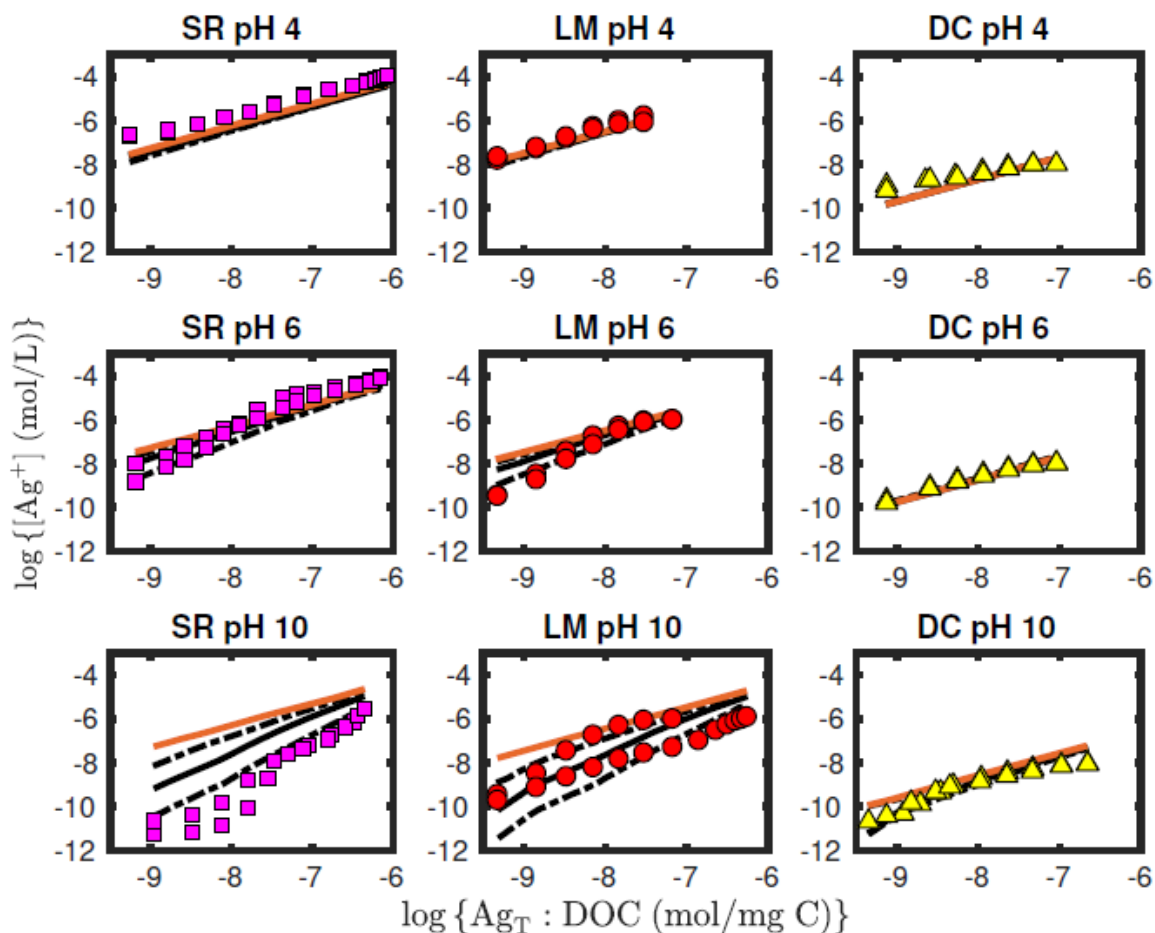


357

358 Figure 3: WHAM predictions of silver binding to the DOM samples at pH 8. Points are
 359 observations (sample legend is given in Figure 1). Black lines are WHAM predictions using
 360 the default assumption of DOM being 65% chemically active as fulvic acid, dashed lines
 361 show predictions with uncertainty of ± 0.3 in the binding constant $\log K_{MA}$ for Ag^+ taken into
 362 account (Ahmed et al., 2013; Lofts and Tipping, 2011). Orange lines show the predicted free
 363 Ag in the absence of DOM, i.e. when complexation is due only to the presence of chloride.
 364 The blue dashed line is the calculated binding curve for cysteine-like sites, determined using
 365 measured CRS as the ligand concentration.

366 3.4. Silver Binding Model for Waste Water

367 Sulphur-based (thiol-type) groups in the samples may be important in binding Ag . To
 368 investigate whether this might be significant, we also ran simulations using cysteine as an
 369 analogue for S-binding moieties. Proton- and Ag binding constants for cysteine were
 370 obtained from the literature (Voronkov et al., 2002; Alekseev et al., 2012). The
 371 corresponding reactions and $\log K$ values are presented in Table 3.



372

373 Figure 4: WHAM predictions of silver binding to the SR, LM and DC DOM samples at pH 4.0,
 374 6.0 and 10.0. Points are observations (colours are as in Figure 1). Black lines are WHAM
 375 predictions using the default assumption of DOM being 65% chemically active as fulvic acid,
 376 dashed lines show predictions with uncertainty of ± 0.3 in the binding constant $\log K_{MA}$ for Ag
 377 taken into account (Ahmed et al., 2013; Lofts and Tipping, 2011). Orange lines show the
 378 predicted free Ag in the absence of DOM, i.e. when complexation is due only to the
 379 presence of chloride.

380 Precipitation of Ag_2S was not included in the modelling because there is no evidence of
 381 silver precipitation other than $AgCl(s)$ which forms at the highest added silver concentrations.
 382 Precipitation of a silver mineral phase would result in a constant $[Ag^+]$ response as is seen
 383 when $AgCl(s)$ forms. The amount of cysteine in simulations was determined from the
 384 measured chromium-reducible sulphur (CRS) in the DOM samples, assuming all the CRS to
 385 have similar binding behaviour to cysteine-type thiol groups (measured thiol, as opposed to
 386 CRS, did not correlate with silver binding (Table S12)). Predictions are shown as the blue line
 387 in Figure 3. In all cases the addition of thiol-type groups increases the predicted
 388 complexation of Ag, as would be expected. However, the agreement between observation

389 and prediction is generally poorer, even where observed complexation is higher than that
 390 predicted in the absence of thiol-type groups. This suggests that although thiol-type groups
 391 may be playing an important role in complexation in some of the DOM samples, the
 392 concentration of thiol-type groups that is actively taking part in binding is lower than the
 393 measured CRS. In samples NR and BB the silver binding predictions are clearly superior
 394 when thiol-type groups are not considered. Thus, for typical surface water samples
 395 assuming that the active silver binding ligands are predominantly fulvic acid-based, WHAM
 396 is an appropriate approach for assessing silver speciation; there is no improvement when
 397 reduced sulphide ligands are considered explicitly using measured CRS concentrations.

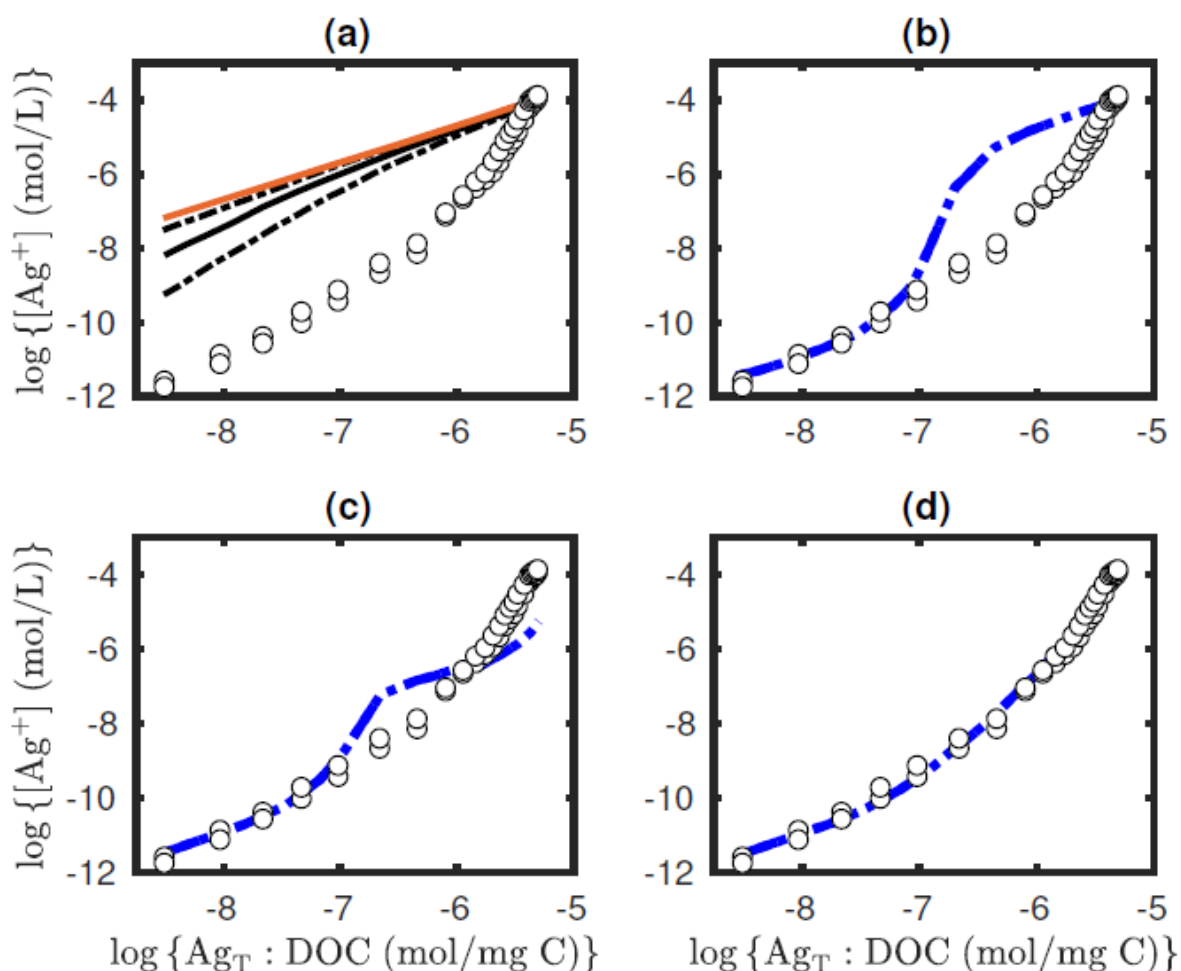
398 Table 3: Formation constants for silver and proton complexation to cysteine (Cys) and
 399 histidine (His) using reactions and logK values from Voronkov et al. (2002) and Alekseev et
 400 al. (2012) for Cys and from Smith and Martell (2004) for His.

Cys Reaction	logK value	His Reaction	logK value
$\text{Cys}^{2-} + \text{H}^+ \rightleftharpoons \text{HCys}^-$	10.37	$\text{His}^- + \text{H}^+ \rightleftharpoons \text{HHis}^0$	9.28
$\text{Cys}^{2-} + 2\text{H}^+ \rightleftharpoons \text{H}_2\text{Cys}$	18.60	$\text{His}^- + 2\text{H}^+ \rightleftharpoons \text{H}_2\text{His}^+$	15.25
$\text{Cys}^{2-} + 3\text{H}^+ \rightleftharpoons \text{H}_3\text{Cys}^+$	20.58	$\text{His}^- + 3\text{H}^+ \rightleftharpoons \text{H}_3\text{His}^{2+}$	16.85
$\text{Cys}^{2-} + \text{Ag}^+ \rightleftharpoons \text{AgCys}^-$	11.14	$\text{His}^- + \text{H}^+ + \text{Ag}^{++} \rightleftharpoons \text{AgHHis}^+$	12.41
$\text{Cys}^{2-} + \text{H}^+ + \text{Ag}^+ \rightleftharpoons \text{AgHCys}$	20.77	$2\text{His}^- + 2\text{H}^+ + \text{Ag}^{++} \rightleftharpoons \text{Ag}(\text{HHis})_2^+$	25.41
$\text{Cys}^{2-} + 2\text{Ag}^+ \rightleftharpoons \text{Ag}_2\text{Cys}$	20.32	$2\text{His}^- + 2\text{H}^+ + 2\text{Ag}^{++} \rightleftharpoons \text{Ag}_2(\text{HHis})_2^{2+}$	34.29
$\text{Cys}^{2-} + \text{H}^+ + 2\text{Ag}^+ \rightleftharpoons \text{Ag}_2\text{HCys}$	27.28		

401

402 For wastewater though, WHAM significantly underpredicts binding. This is not at all
 403 surprising given that WHAM was calibrated for freshwater organic matter with low nitrogen
 404 and sulphur content. Figure 5(a) shows WHAM predictions for the UW raw sewage sample.
 405 The complexation of silver by the sample is clearly greater than can be predicted from the
 406 chemistry of humic substances. For the UW sample a calculation of the amount of silver
 407 bound per g of organic matter reveals that the bound Ag exceeds $0.001 \text{ mol g DOM}^{-1}$. This
 408 demonstrates that the UW DOM has an unusually high binding capacity compared to humic
 409 material; for example, SR at pH 8.0 has a capacity of approximately $10^{-5} \text{ mol g DOM}^{-1}$. This
 410 suggests strongly that the DOM in the UW sample is dominated not by humic-type material
 411 but by material with a high Ag binding strength and capacity, such as reduced sulphur and/or
 412 proteinaceous materials. These materials could include inorganic colloidal materials (i.e.,
 413 metal sulphides) associated with the DOM.

414 Predicted Ag complexation in the presence of groups with thiol-type binding strength is
 415 shown in Figure 5(b). Assuming the presence of reduced sulphur groups gives a somewhat
 416 improved prediction, with excellent agreement at low Ag loading (up to $\log(\text{Ag}_T:\text{DOC}) \sim 5.8$).
 417 However, at higher Ag loadings binding remains under predicted by a considerable margin.
 418 This suggests that while binding to thiol-type groups is sufficient to explain binding at the low
 419 end of the Ag loading range, additional binding sites are required to provide a full description
 420 of the overall complexation behaviour. Given the high overall binding capacity, which cannot
 421 be explained by binding to humic-type material, the most likely explanation is the presence
 422 of additional nitrogenous groups on proteinaceous material.



423
 424 Figure 5: (a) WHAM predictions of silver binding to the UW sample at pH 8. Black lines are
 425 WHAM predictions using the default assumption of DOM being 65% chemically active as
 426 fulvic acid, dashed lines show predictions with uncertainty of ± 0.3 in the binding constant
 427 $\log K_{MA}$ for Ag taken into account (Ahmed et al., 2013; Lofts and Tipping, 2011). Orange lines
 428 show the predicted free Ag in the absence of DOM, i.e. when complexation is due only to the
 429 presence of chloride. Open circles are the measured UW titration data. (b) Observed (open
 430 symbols) and predicted (blue line) Ag complexation in the UW sample, assuming the

431 presence of thiol-type groups (Table 3). (c) Observed (open symbols) and predicted (blue
432 line) Ag complexation in the UW sample, assuming the presence of thiol-type groups as well
433 as amine groups. (d) Observed (open symbols) and predicted (blue line) Ag complexation in
434 the UW sample, using a best-fit empirical model (Table 3).

435 To test the possible contribution from nitrogenous binding sites, the C:N ratio of the DOM in
436 raw sewage was first estimated. There is a wide literature on the composition of raw
437 sewage, presenting a range of possible C:N ratios. For example, Gray (2004) gives a C:N
438 ratio of raw sewage of 100:17 (5.9), giving an estimated N content for the UW sample of
439 1350 nmol N/mg C. To probe the possible influence of nitrogenous groups, we assumed this
440 N to be present as histidine. Equilibrium constants (see Table 3) for proton and silver binding
441 to histidine were added to WHAM and the model results shown in Fig 5(c). All binding data
442 were taken from Smith and Martell (2004). Figure 5(c) shows the outcome of a prediction
443 using 100 nmol S/mg C (cf. Figure 5(b)) and 1350 nmol N/mg C. The addition of histidine to
444 represent amino N groups improves the prediction compared to that when thiol groups only
445 are represented. However, the combination of ligands cannot represent the observed shape
446 of the titration curve, since they do not provide enough binding heterogeneity.

447 An alternative approach to representing binding sites by a collection of small ligands of
448 known chemistry is to represent silver binding to a collection of ligands, assuming a simple
449 1:1 reaction stoichiometry (as shown in Equation 3), and to fit binding strengths and site
450 densities directly to the data.



452 This approach has the advantage of allowing an optimal description of the binding
453 behaviour, at the expense of a level of realism in terms of ligand identity. To permit the fitting
454 of a multiligand model with a reasonable number of parameters, we used a formulation
455 whereby the binding strengths (logK values) and site densities (S, mmol/g) were related to
456 each other. We postulated a collection of n ligands denoted L₁, L₂, ... L_n. Defining the silver
457 binding strength and site density of L₁ as logK₁ and [S₁], we then define the binding
458 strengths and site densities of the remaining ligands in relation to the values for L₁:

$$459 \log K_x = \log K_1 + (x - 1) \cdot \Delta \log K \quad (4)$$

$$460 [S_x] = [S_1] \cdot \Delta [S]^{x-1} \quad (5)$$

461 where x is the ligand number (x = 2, ..., n) and logK and [S] are fitting parameters. This
462 scheme allows fitting of any number of ligands greater than one using four binding
463 parameters. The number of ligands required must be set *a priori* by fixing n at different
464 values and optimizing the four adjustable parameters (logK₁, [S₁], ΔlogK and Δ[S]). The

465 optimal number of sites is that above which adding another site does not produce a
 466 significant improvement in the fit. For the WS data fitting trials suggested that the optimal
 467 number of sites was five. Fitting produced the optimal parameter values given in Table 4 and
 468 the optimal fit shown in Figure 5(d). The five-site model gives an excellent fit to the data,
 469 emphasizing that such a degree of heterogeneity is needed to describe the trend in silver
 470 binding. The binding strength of site number 1 (the strongest) is reasonably close to that for
 471 1:1 binding of silver to cysteine ($\text{Ag}^+ + \text{HCys}^- = \text{AgHCys}^0$; $\log K = 11.37$ when $I = 0.01$ mol/L).
 472 However, the binding strengths of the remaining sites are stronger than those for silver
 473 binding to amino groups, e.g. on histidine ($\text{Ag}^+ + \text{HHis}^- = \text{AgHHis}^0$; $\log K = 3.13$ when $I = 0.01$
 474 mol/L). This suggests that other types of sites, such as multidentate sites comprising two or
 475 three amino N groups, might be important for silver binding. Such sites would be expected to
 476 have $\log K$ values for 1:1 binding in the range ~6-9, i.e. approximately double to triple the 1:1
 477 binding affinity for silver to histidine.

478 Table 4: Optimised parameters for the multiligand model, fitted to the WS sewage titration.
 479 The $\log K$ values are conditional for the ionic strength of the WS titration ($I = 0.01$ mol/L).

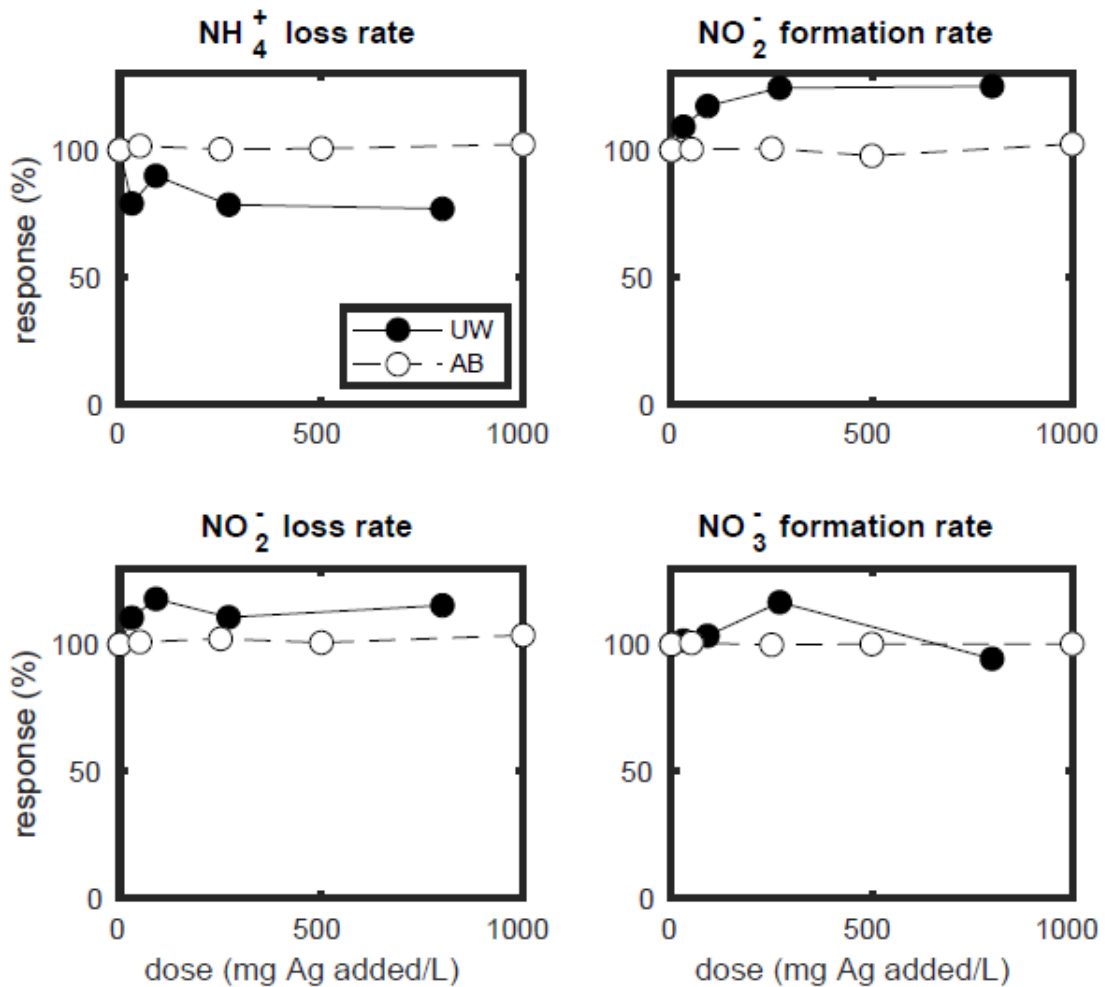
Parameter	Optimized value
$\log K_1$	10.24
$\Delta \log K$	-1.15
[S1] nmol/mg C	66.7
$\Delta[S]$	2.24
$\log K_2$	9.09
$\log K_3$	7.94
$\log K_4$	6.79
$\log K_5$	5.64
[S2] nmol/mg C	149
[S3] nmol/mg C	334
[S4] nmol/mg C	749
[S5] nmol/mg C	1679

480

481 3.5. Silver toxicity to N oxidizing bacteria in sewage, range finder experiment

482 In wastewater treatment, organic ligands (DOM) that have the potential to complex with
 483 silver, may originate in the raw wastewater or may be generated as soluble microbial
 484 products (SMP). The chelating properties of SMP have been attributed to various functional
 485 groups including carboxylates, hydroxyls, thiols, phenols and amines (Kuo and Parkin,
 486 1996). Holakoo et al. (2006) found that SMP were moderate chelators of copper as indicated

487 by logK values of 7.6-8.8 and 6.3-6.8 for moderate and weaker ligands, respectively. Weaker
 488 ligands contributed more than half of the total ligand concentration. SMP with molecular
 489 weights of 1-10 kD were found to have the highest complexation capacity among all the
 490 SMP fractions. SMPs are expected to complex silver and reduce silver toxicity to
 491 microorganisms in the wastewater matrix.



492
 493 Figure 6: Dose response curves for nitrogen redox transformations in aerated raw sewage
 494 from two sources. The silver dose is recorded as the nominal amount of silver added.

495 SMP are released by microorganisms during substrate metabolism, biomass growth, and
 496 biomass decay, and constitute a major part of the residual organic matter in the e uent from
 497 biological wastewater treatment plants (Kunacheva and Stuckey, 2014; Xie et al., 2016).
 498 SMP comprise a wide range of high and low molecular weight compounds including
 499 proteins, polysaccharides, humic and fulvic acids, nucleic acids, enzymes and structural
 500 compounds (Rittmann et al., 1987; Parkin and McCarty, 1981). Xie et al. (2016) identified
 501 solids retention time, influent chemical oxygen demand (COD) concentration and hydraulic
 502 retention time as factors influencing SMP formation in wastewater treatment plants. While,

503 Hu et al. (2019) demonstrated that the effect of temperature on the chemical characterization
504 of soluble dissolved nitrogen was different from that of soluble dissolved carbon, and hence
505 the composition of SMPs changed with temperature. Thus, the release of ligands that could
506 bind metals in receiving waters will likely vary with location and season; thus, two sources of
507 sewage were studied (see below).

508 A simple range finder experiment was designed to test the impacts of silver on ammonia
509 oxidation to nitrate with nitrite as an intermediate species; Figures SI2 and SI3 show the
510 experimental setup. Measurements of the concentration of each nitrogen species
511 concentration versus time show the expected trend of ammonia transformation to nitrite and
512 subsequently nitrite transformation to nitrate (Figure SI5 for the UW sample and SI6 for the
513 Ash AB sample). From the species data alone it is hard to discern if there is any e
514 ffect of the added silver; the data look very similar. To probe the data further the rates of
515 transformations of each species were calculated from the slopes of each species
516 concentration versus time. In this way rate of NH_4^+ loss, NO_2^- formation and loss and NO_3^-
517 formation were calculated (Figure 6).

518 There were replicate flasks during the oxidation tests but there were analytical issues and
519 some of the replicate analyses were lost. Figures SI5 and SI6 show what replicate data was
520 available as duplicate data points; for the majority of treatments and times only one data
521 point was measured. This lack of available replicate data makes it impossible to report actual
522 effect concentrations. Still, inspection of Figure 6 reveals that the effects are no greater than
523 20% even up to 1000 $\mu\text{g Ag/L}$. The Ashbridges Bay sewage sample (AB) actually shows
524 very minimal variations (less than 5%) with respect to added silver. The UW sample
525 suggests a slowing of about 20% on ammonia loss rates and nitrite formation rates.
526 Similarly, nitrite loss and nitrate formation rates increase by less than 20%.

527 A previous sediment incubation study on nitrogen oxidation kinetics showed that silver
528 nanoparticles only impacted N_2O production at high silver doses. Zheng et al. (2017)
529 determined that N_2O production was stimulated by silver nanoparticles in estuarine
530 sediments at doses of <534, 1476, 2473 $\mu\text{g/L}$ for 10, 30 and 100 nm sized silver
531 nanoparticles respectively. A study on wastewater biofilms by Sheng et al. (2015)
532 demonstrated that at 200 mg Ag/L silver doses, as silver nanoparticles, silver decreased
533 community diversity but did not significantly affect microbial community function. Sheng et al.
534 (2015) did not investigate any other silver concentrations, and such a high dose is much
535 larger than could reasonably be achieved by discharge of personal care products; Ag
536 concentrations in personal care products has been reported to be between 17 to 30 mg
537 kg^{-1} (Khaksar et al., 2019). The research presented in this current paper, although at much

538 lower total silver doses did not investigate impacts on community diversity though, and this
539 should be addressed in follow-up studies. There would be the potential for negative impacts
540 if bacterial community diversity were to be modified in a receiving water (Zeglin, 2015).

541 Dissolved organic carbon also showed no trends with respect to nominal silver dose (Figure
542 SI7). The DOC did decrease with time from 35 to approximately 10 over 30 days consistent
543 with degradation of organic matter in the raw sewage, but there was no influence of silver
544 dose on the DOC degradation kinetics. Dissolved silver decreased rapidly in all exposures
545 (Figure SI8); by day 18 there was no detectable dissolved silver remaining in solution for any
546 of the treatments. The removal of silver was likely due to sulphide precipitation and this
547 removal would be protective with respect to the bacterial community. The complexation in
548 solution would also render the remaining soluble silver less bioavailable.

549 The sewage incubation experiments also allowed testing of the hypothesis that sewage
550 organic matter would become more “WHAM-like” as it oxidized; i.e., the silver binding
551 properties of the aged material became more similar to WHAM predictions of humic
552 substance silver complexation. From the Ash AB control incubations subsamples were taken
553 for silver titration at day 0, 2, 15, 18 and 30 (Figure SI9). The youngest two samples showed
554 the strongest binding; i.e., the lowest free silver concentrations. The three later samples
555 were an order of magnitude higher in initial free silver concentrations. The measured values
556 are still 3 orders of magnitude lower than WHAM predictions, but the tendency is towards
557 binding curves more closely resembling allochthonous organic matter, suggesting that the
558 very strong silver binding ligands are effectively reduced by wastewater treatment.

559 4. Conclusions

560 WHAM predicts silver speciation very well within the model confidence envelope using DOC
561 as the input variable across pH values from 4 to 10. There are almost two orders of
562 magnitude variation in free silver between sources but, within model uncertainty, WHAM
563 captures this variability. Thus for risk assessment WHAM is an appropriate tool for predicting
564 silver speciation in surface waters.

565 The raw sewage sample tested was not modelled correctly by WHAM though. Investigation
566 of the data suggested that the binding strength and capacity was much greater than that of
567 humic-type material. We suggest that this is due to ligands derived from components of raw
568 sewage, such as a proteinaceous material, that we would expect to be at low concentrations
569 in natural waters unimpacted by raw sewage. WHAM simulations with thiol-type binding sites
570 could explain the binding of silver at low loadings but not at higher loadings. This suggests
571 the presence of an additional class or classes of strongly binding ligands, possibly nitrogen-
572 based groups.

573 This project involved testing the performance of existing software (Windermere Humic
574 AqueousModel (WHAM)) for predicting the forms of silver in receiving waters. It was found
575 that this software performs very well for most surface freshwater environments. The only
576 time the model overpredicts the amount of toxic free silver ion is in heavily sewage impacted
577 environments. This additional binding not captured by the modelling means that any
578 management decisions performed using WHAM would be conservative though. Thus, silver
579 stakeholders can proceed with WHAM-based risk assessment. An early prototype sewage-
580 specific silver prediction model has been developed as part of this project. Such a model can
581 serve as a useful starting point for a more comprehensive model taking other variables, such
582 as pH, into account, and specifically a revised modelling approach would relate independent
583 measures of DOM quality to ligand concentrations, rather than fitting these values for a
584 specific “batch” of sewage, as was done here. Ultimately, such a model would be of great
585 use to stakeholders, as a means to perform silver risk assessment for sewage-impacted
586 waters.

587 In addition, after it was found that WHAM did not predict silver binding in sewage,
588 wastewater was explored further in incubation experiments to test if sewage would become
589 more like humic substances with age and if silver would impact the natural treatment of
590 sewage by bacteria. It was found that sewage does become more WHAM like with age but
591 even after a month binds silver more strongly than organic matter from natural aquatic
592 environments. Silver did not impact the natural attenuation of sewage though and it seems
593 that silver-containing products do not cause unanticipated consequences in regions of low
594 wastewater treatment technology.

595 5. Acknowledgements

596 Funding was provided by Unilever and Unilever Canada, as well as the NSERC CRD
597 program. Also thank you to Taylor Dunn and Sam Smith for their assistance with BB and DC
598 sample collection; best field assistants ever!

599 References

- 600 Adams, W., Blust, R., Dwyer, R., Mount, D., Nordheim, E., Rodriguez, P.H., Spry, D., 2019.
601 Bioavailability assessment of metals in freshwater environments: A historical review.
602 *Environmental Toxicology and Chemistry* 39, 48–59. doi:10.1002/etc.4558.
- 603 Ahmed, I.A., Hamilton-Taylor, J., Lofts, S., Meeussen, J.C.L., Lin, C., Zhang, H., Davison,
604 W., 2013. Testing copper-speciation predictions in freshwaters over a wide range of metal–
605 organic matter ratios. *Environmental Science & Technology* ,
606 130118162041009doi:10.1021/402 es304150n.

607 Al-Reasi, H., Smith, D.S., Wood, C.M., 2011a. Evaluating the ameliorative e
608 ect of natural dissolved organic matter (DOM) quality on copper toxicity to aquatic
609 organisms: Improving the BLM. *Ecotoxicology* 21, 524–537. doi:10.1007/s10646-011-0813-
610 z.

611 Al-Reasi, H.A., Wood, C.M., Smith, D.S., 2011b. Physicochemical and spectroscopic
612 properties of natural organic matter (NOM) from various sources and implications for
613 ameliorative effects on metal toxicity to aquatic biota. *Aquatic Tox.* 103, 179–190.
614 doi:10.1016/j.aquatox.2011.02.015.

615 Alekseev, V.G., Semenov, A.N., Pakhomov, P.M., 2012. Complexation of Ag⁺ ions with L-
616 cysteine. *Russian Journal of Inorganic Chemistry* 57, 1041–1044.
617 doi:10.1134/s0036023612070029.

618 Bowles, K.C., Ernste, M.J., Kramer, J.R., 2003. Trace sulfide determination in oxic
619 freshwaters. *Anal. Chim. Acta* 477, 113–124. doi:10.1016/S0003-2670(02)01370-3.

620 Brauner, C., Wood, C.M., 2002. Ionoregulatory development 412 and the effect of chronic
621 silver exposure on growth, survival, and sublethal indicators of toxicity in early life stages of
622 rainbow trout (*oncorhynchus mykiss*). *Journal of Comparative Physiology B: Biochemical,*
623 *Systemic, and Environmental Physiology* 172, 153–162. doi:10.1007/s00360-001-0238-8.

624 Carvalho, R.N., Marinov, D., Loos, R., Napierska, D., Chirico, N., Lettieri, T., 2016.
625 Monitoring-based exercise: Second review of the priority substances list under the water
626 framework directive. monitoring-based exercise. Joint Research Centre, Institute for
627 Environment and Sustainability, Water Resources Unit TP.

628 Cooper, C., Tait, T., Gray, H., Cimprich, G., Santore, R., McGeer, J.C., Wood, C., Smith,
629 D.S., 2014. Influence of salinity and dissolved organic carbon on acute Cu toxicity to the
630 rotifer *Brachionus plicatilis*. *Environ. Sci. Technol.* 48, 1213–1221. doi:10.1021/es402186w.

631 Curtis, P.J., Schindler, D.W., 1997. Hydrologic control of dissolved organic matter in low-
632 order precambrian shield lakes. *Biogeochemistry* 36, 125–138.
633 doi:10.1023/a:1005787913638.

634 De Schamphelare, K.A., Vasconcelos, F.M., Tack, F.M.G., Allen, H.E., Janssen, C.R., 2004.
635 Effect of dissolved organic matter source on acute copper toxicity to *Daphnia magna*.
636 *Environ. Toxicol. and Chem.* 23, 1248–1255. doi:10.1897/03-184.

637 Di Toro, D., Allen, H., Bergman, H., Meyer, J., Paquin, P., Santore, R., 2001. Biotic ligand
638 model of the acute toxicity of metals I : Technical basis. *Environ. Toxicol. Chem.* 20, 2383–
639 2396. doi:10.1002/etc.5620201034.

640 Emam, H.E., Manian, A.P., Široka, B., Duelli, H., Redl, B., Pipal, A., Bechtold, T., 2013.
641 Treatments to impart antimicrobial activity to clothing and household cellulosic-textiles – why
642 “nano”-silver? *Journal of Cleaner Production* 39, 17–23. doi:10.1016/j.jclepro.2012.08.038.

643 Environment Agency, 2009. Using biotic ligand models to help implement environmental
644 quality standards for metals under the water framework directive. URL:
645 [https://www.wfduk.org/sites/default/files/Media/Environmental%20standards/biotic%20ligand](https://www.wfduk.org/sites/default/files/Media/Environmental%20standards/biotic%20ligand%20models%20implement%20EQS.pdf)
646 [%20models%20implement%20EQS.pdf](https://www.wfduk.org/sites/default/files/Media/Environmental%20standards/biotic%20ligand%20models%20implement%20EQS.pdf). Science Report SC080021/SR7b, Environment
647 Agency, Bristol, UK.

648 European Commission (EC), 2013. Directive 2013/39/eu of the european parliament and of
649 the council of 12 august 2013 amending directives 432 2000/60/ec and 2008/105/ec as
650 regards priority substances in the field of water policy. URL: [http://eur-lex.europa.eu/legal-](http://eur-lex.europa.eu/legal-content/EN/TXT/PDF/?uri=CELEX:32013L0039&from=EN)
651 [content/EN/TXT/PDF/?uri=CELEX:32013L0039&from=EN](http://eur-lex.europa.eu/legal-content/EN/TXT/PDF/?uri=CELEX:32013L0039&from=EN). Official Journal of the European
652 Union, 24.8.2013.

653 European Commission (EC), 2018. Common implementation strategy for the water
654 framework directive (2000/60/EC) revised guidance document no. 27 technical guidance for
655 deriving environmental quality standards. European Communities.

656 Gray, N.F., 2004. *Biology of wastewater treatment*. Imperial College Press, London.

657 Hiriart-Baer, V., Fortin, C., Lee, D., Campbell, P., 2006. Toxicity of silver to two freshwater
658 algae, *Chlamydomonas reinhardtii* and *Pseudokirchneriella subcapitata*, grown under
659 continuous culture conditions: Influence of thiosulphate. *Aquatic Toxicology* 78, 136–148.
660 doi:10.1016/j.aquatox.2006.02.027.

661 Hites, R.A., 2019. Correcting for censored environmental measurements. *Environmental*
662 *Science & Technology* 53, 11059–11060. doi:10.1021/acs.est.9b05042.

663 Hogstrand, C., Galvez, F., Wood, C.M., 1996. Toxicity, silver accumulation and
664 metallothionein induction in sewage effluent impacted waters by competitive ligand titration
665 with silver. *Environ. Sci. Technol* 38, 2120–2125. doi:10.1002/etc.5620150713.

666 Holakoo, L., Nakhla, G., Yanful, E.K., Bassi, A.S., 2006. Chelating properties and molecular
667 weight distribution of soluble microbial products from an aerobic membrane bioreactor.
668 *Water Research* 40, 1531–1538. doi:10.1016/j.watres.2006.02.002.

669 Hu, H., Shi, Y., Liao, K., Ma, H., Xu, K., Ren, H., 2019. Effect of temperature on the
670 characterization of soluble microbial products in activated sludge system with special
671 emphasis on dissolved organic nitrogen. *Water Research* 162, 87–94.
672 doi:10.1016/j.watres.2019.06.034.

673 Johnson, A.C., Jürgens, M.D., Lawlor, A.J., Cisowska, I., Williams, R.J., 2014. Particulate
674 and colloidal silver in sewage effluent and sludge discharged from British wastewater
675 treatment plants. *Chemosphere* 112, 49–55. doi:10.1016/j.chemosphere.2014.03.039.

676 Khaksar, M., Vasileiadis, S., Sekine, R., Brunetti, G., Scheckel, K.G., Vasilev, K., Lombi, E.,
677 Donner, E., 2019. Chemical characterisation, antibacterial activity, and (nano)silver
678 transformation of commercial personal care products exposed to household greywater.
679 *Environmental Science: Nano* 6, 3027–3038. doi:10.1039/c9en00738e.

680 Kunacheva, C., Stuckey, D.C., 2014. Analytical methods for soluble microbial products
681 (SMP) and extracellular polymers (ECP) in wastewater treatment systems: A review. *Water*
682 *Research* 61, 1–18. doi:10.1016/j.watres.2014.04.044.

683 Kuo, W.C., Parkin, G.F., 1996. Characterization of soluble microbial products from anaerobic
684 treatment by molecular weight distribution and nickel-chelating properties. *Water Research*
685 30, 915–922. doi:10.1016/0043-1354(95)00201-4.

686 Lofts, S., Tipping, E., 2011. Assessing WHAM/Model VII against field measurements of free
687 metal ion concentrations: model performance and the role of uncertainty in parameters and
688 inputs. *Environmental Chemistry* 8, 501. doi:10.1071/en11049.

689 McKnight, D.M., Boyer, E.W., Westerhoff, P.K., Doran, P.T., Kulbe, T., Andersen, D.T.,
690 2001. Spectrofluorimetric characterization of dissolved organic matter for indication of
691 precursor organic material and aromaticity. *Limnol. Oceanog.* 46, 38–48.

692 Merrington, G., Peters, A., Schlegel, C.E., 2016. Accounting for metal bioavailability in
693 assessing water quality: A step change? *Environmental Toxicology and Chemistry* 35, 257–
694 265. doi:10.1002/etc.3252.

695 Naddy, R.B., Stubblefield, W.A., Bell, R.A., Wu, K.B., Santore, R.C., Paquin, P.R., 2017.
696 Influence of varying water quality parameters on the acute toxicity of silver to the freshwater
697 cladoceran, *ceriodaphnia dubia*. *Bulletin of Environmental Contamination and Toxicology*
698 100, 69–75. doi:10.1007/s00128-017-2260-x.

699 Nadella, S.R., Tellis, M., Diamond, R.L., Smith, D.S., Bianchini, A., Wood, C.M., 2013.
700 Toxicity of lead and zinc to developing mussel and sea urchin embryos: Critical tissue
701 residues and effects of dissolved organic matter and salinity. *Comp. Biochem. Biophys. C*
702 158, 72–83. doi:10.1016/j.cbpc.2013.04.004.

703 Parkin, G., McCarty, P., 1981. A comparison of the characteristics of soluble organic nitrogen
704 in untreated and activated sludge treated wastewaters. *Water Research* 15, 139–149.
705 doi:10.1016/0043-1354(81)90194-9.

706 Peters, A., Simpson, P., Merrington, G., Rothenbacher, K., Sturdy, L., 2011. Occurrence and
707 concentration of dissolved silver in rivers in England and Wales. *Bulletin of Environmental*
708 *Contamination and Toxicology* 86, 637–641. doi:10.1007/s00128-011-0288-x.

709 Rader, K.J., Shadi, T.S., Mahony, J.D., Toro, D.M.D., 2005. Measuring the partitioning of
710 silver to organic carbon using solubility enhancement. *Environmental Toxicology and*
711 *Chemistry* 24, 2833. doi:10.1897/04-577r.1.

712 Rittmann, B.E., Bae, W., Namkung, E., Lu, C.J., 1987. A critical evaluation of microbial
713 product formation in biological processes. *Water Science and Technology* 19, 517–528.
714 doi:10.2166/wst.1987.0231.

715 Sahlin, S., Ågerstrand, M., 2018. Silver: EQS data overview. ACES Report Number 30. URL:
716 [https://www.aces.su.se/aces/wp-content/uploads/2018/10/Silver-EQS-data-overview-](https://www.aces.su.se/aces/wp-content/uploads/2018/10/Silver-EQS-data-overview-2018.pdf)
717 [2018.pdf](https://www.aces.su.se/aces/wp-content/uploads/2018/10/Silver-EQS-data-overview-2018.pdf). Report undertaken on behalf of the Swedish Agency of Marine and Water
718 Management and the Swedish Environmental Protection Agency. Pp. 31.

719 Schwartz, M.L., Curtis, P.J., Playle, R.C., 2004. Influence of natural organic matter source
720 on acute copper, lead, and cadmium toxicity to rainbow trout *Oncorhynchus mykiss*. *Environ.*
721 *Toxicol. Chem.* 23, 2889–2899. doi:10.1897/03-561.1.

722 Sheng, Z., Nostrand, J.D.V., Zhou, J., Liu, Y., 2015. The effects of silver nanoparticles on
723 intact wastewater biofilms. *Frontiers in Microbiology* 6. doi:10.3389/fmicb.2015.00680.

724 Sikora, F., Stevenson, F., 1988. Silver complexation by humic substances: conditional
725 stability constants and nature of reactive sites. *Geoderma* 42, 353–363.

726 Smith, D.S., Bell, R.A., Valliant, J., Kramer, J.R., 2004. Determination of strong ligand sites
727 in sewage effluent-impacted waters by competitive ligand titration with silver. *Environmental*
728 *Science & Technology* 38, 2120–2125. doi:10.1021/es035045p.

729 Smith, R.M., Martell, A.F., 2004. Nist critically selected stability of metal complexes
730 database. nist standard reference database 46. National Institute of Standards and
731 Technology, Gaithersburg, MD, U.S.A.

732 Sun, L., Perdue, E., McCarthy, J., 1995. Using reverse osmosis to obtain organic matter
733 from surface and ground waters. *Water Research* 29, 1471–1477. doi:10.1016/0043-
734 1354(94)00295-i.

735 Tait, T.N., Rabson, L.M., Diamond, R.L., Cooper, C.A., McGeer, J.C., Smith, D.S., 2015.
736 Determination of cupric ion concentrations in marine waters: an improved procedure and
737 comparison with other speciation methods. *Env. Chem.* 13, 140–148. doi:10.1071/EN14190.

738 Tipping, E., Lofts, S., Sonke, J.E., 2011. Humic ion-binding Model VII: a revised
739 parameterisation of cation-binding by humic substances. *Environmental Chemistry* 8, 225.
740 doi:10.1071/en11016.

741 Voronkov, M.G., Antonik, L.M., Kogan, A.S., Lopyrev, V.A., Fadeeva, T.V., Marchenko, V.I.,
742 Abzaeva, K.A., 2002. Antimicrobial and hemostatic effects of silver salts of poly(acrylic acid).
743 *Pharmaceutical Chemistry Journal* 36, 26–28. doi:10.1023/a:1016059914046.

744 Wakshlak, R.B.K., Pedahzur, R., Avnir, D., 2015. Antibacterial activity of silver-killed
745 bacteria: the “zombies” effect. *Scientific Reports* 5, 1–5. URL:
746 <http://dx.doi.org/10.1038/srep09555>.

747 Winter, A., Fish, T., Playle, R., Smith, D.S., Curtis, P., 2007. Photodegradation of natural
748 organic matter from diverse freshwater sources. *Aquat. Toxicol.* 84, 215–222.
749 doi:10.1016/j.aquatox.2007.04.014.

750 Xie, W.M., Ni, B.J., Sheng, G.P., Seviour, T., Yu, H.Q., 2016. Quantification and kinetic
751 characterization of soluble microbial products from municipal wastewater treatment plants.
752 *Water Research* 88, 703–710. doi:10.1016/j.watres.2015.10.065.

753 Zeglin, L.H., 2015. Stream microbial diversity in response to environmental changes: review
754 and synthesis of existing research. *Frontiers in Microbiology* 6.
755 doi:10.3389/fmicb.2015.00454.

756 Zheng, Y., Hou, L., Liu, M., Newell, S.E., Yin, G., Yu, C., Zhang, H., Li, X., Gao, D., Gao, J.,
757 Wang, R., Liu, C., 2017. Effects of silver nanoparticles on nitrification and associated nitrous
758 oxide production in aquatic environments. *Science Advances* 3, e1603229.
759 doi:10.1126/sciadv.1603229.